NASA
Technical
Paper
2373
C.1
January 1985

Reduction Method for Thermal Analysis of Complex Aerospace Structures

Charles P. Shore

NASA

NASA
Technical
Paper
2373

1985

Reduction Method for Thermal Analysis of Complex Aerospace Structures

Charles P. Shore

Langley Research Center
Hampton, Virginia

NASA
National Aeronautics
and Space Administration

Scientific and Technical
Information Branch

Introduction

Although intensive research efforts into improved numerical methods and programing techniques for nonlinear structural analyses have led to many advances in the solution of large-scale structural analyses, such problems continue to require large amounts of computer resources. The large numbers of degrees of freedom required in complex structural models often result from modeling structural topology rather than complexity of structural behavior. Recognition of this fact has led to considerable research into methods to reduce the degrees of freedom in structural problems and, hence, reduce the required computer resources. These methods have become known as reduction methods and are thoroughly reviewed in reference 1. Reduction methods transform the unknown nodal degrees of freedom of finite-element structural models (full system) to a smaller set of unknown parameters or generalized coordinates of the reduced system of equations. The link between the full and reduced systems of equations is a transformation matrix. The columns of the transformation matrix are referred to as reduced basis vectors. Reduction techniques used in static and dynamic problems combine the classical Rayleigh-Ritz modal superposition methods with contemporary finite-element methods to retain modeling versatility as the number of degrees of freedom is reduced. References 1 to 3 cite several dynamic-response problems for which decreases of over an order of magnitude in the number of degrees of freedom were achieved with the reduction method.

Modal superposition techniques have recently been applied to nonlinear thermal problems. A reduction method which combines the finite-element method with the Galerkin technique is described in reference 4, and a hybrid numerical technique which combines perturbation methods and the classical Bubnov-Galerkin technique is described in reference 5 for steady-state thermal problems. Application of classical modal superposition techniques to transient thermal problems is described in references 6 through 8. However, for nonlinear transient thermal analysis, the classical techniques can require frequent updating of the thermal mode shapes and eigenvalues (decay constants, ref. 6). Reference 9 presents a way of circumventing the updating problem. The idea is based on the reduction technique for dynamic-response problems (refs. 1 to 3) and uses eigenvectors from linear thermal eigenvalue problems for the basis vectors. For the one-dimensional thermal-response problem considered in reference 9, a set of reduced basis vectors selected from eigenvectors corresponding to initial temperature conditions in the structure was found to give excellent agreement while achieving a reduction by a factor of 2 in the number of degrees of freedom. The technique was extended to two-dimensional thermal-response problems in reference 10, where reductions in problem size by a factor of 4 were achieved with errors in nodal temperatures of about 6 percent relative to results from the full-system (unreduced) problem.

This paper describes the reduction method for transient thermal analysis and discusses some recent refinements which have led to improved accuracy with slightly larger reductions in problem size than those achieved in reference 10. Numerical results are presented for two realistic aerospace structures. The first problem represents reentry heating on a segment of the Shuttle wing (see refs. 11 and 12) and is dominated by the conduction characteristics of the Shuttle wing structure and thermal protection system. The second problem represents orbital heating on a large space antenna reflector (described in ref. 13) with essentially negligible conduction effects but with sufficient thermal mass to require a transient solution for accurate prediction of temperatures within the structure. Results from these problems are presented to assess the effectiveness (in terms of the reduction in the number of degrees of freedom only) of the current implementation of the reduction method for thermal analysis of complex aerospace structures.

Symbols and Abbreviations

$[C],[\overline{C}]$	capacitance matrices of full and reduced systems of equations, respectively
c_p	specific heat
DOF	degrees of freedom
FRSI	flexible reusable surface insulation
HRSI	high-temperature reusable surface insulation
h	effective structural thickness
$[K],[\overline{K}]$	conductance matrices of full and reduced systems of equations, respectively
LRSI	low-temperature reusable surface insulation
MRS	microwave radiometer spacecraft
m	number of nodal temperatures
n	number of generalized coordinates or basis vectors
Q	heating rate
$\{Q\},\{\overline{Q}\}$	applied heating vectors of full and reduced systems of equations, respectively
Q_0	temporal distributions (see fig. 4)
RTV	room temperature vulcanized

SIP	strain isolator pad
T	temperature
$\{T\}$	vector of nodal temperatures
$\{\overset{*}{T}\}$	eigenvector from thermal eigenvalue problem (see eq. (3))
t	time
WS	wing station
$x,y,z,$	Cartesian coordinates
$[\Gamma]$	transformation matrix of reduced basis vectors
ε	emissivity
λ	thermal eigenvalue
$\{\psi\}$	vector of generalized coordinates for reduced system of equations

Subscripts:

avg	average
max	maximum

Reduction Method for Transient Thermal Problems

Theory

The system of matrix equations from a finite-element analysis of heat transfer in a structure may be written as follows:

$$\underset{m,m}{[K]}\ \underset{m}{\{T\}} + \underset{m,m}{[C]}\ \underset{m}{\{\dot{T}\}} = \underset{m}{\{Q\}} \tag{1}$$

where $[K]$ is a conductance matrix for the structure, $\{T\}$ is the vector of m unknown nodal temperatures, $[C]$ is the capacitance matrix, $\{\dot{T}\}$ is the time rate of change in the nodal temperatures, and $\{Q\}$ is the applied heat load. The elements of $[K]$ and $[C]$ may be functions of temperature, and the heat load is time dependent. Nodal temperatures from the full system of equations (eq. (1)) may be approximated as functions of the generalized coordinates of a reduced system of equations, as follows:

$$\underset{m}{\{T\}} = \underset{m,n}{[\Gamma]}\ \underset{n}{\{\psi\}} \tag{2}$$

where $[\Gamma]$ is a transformation matrix, and $\{\psi\}$ is a vector of the n unknown generalized coordinates. It is assumed that the local temperature field can be represented by a few assumed temperature distributions or reduced basis vectors, so that n will be much smaller than m. For the procedure described herein, the columns of $[\Gamma]$ (reduced basis vectors) typically are obtained from the solution of two thermal eigenvalue problems associated with equation (1).

However, for some problems, it is necessary to include additional reduced basis vectors from alternate sources, as described in subsequent sections of this report, to obtain accurate results. To form the eigenvalue problems, $\{Q\}$ is taken as zero in equation (1), and $\{T\}$ is assumed to be given by

$$\{T\} = \{\overset{*}{T}_i\}e^{-\lambda_i t} \tag{3}$$

Substitution of the expression for $\{T\}$ from equation (3) into equation (1) results in the following eigenvalue problem:

$$[K]\{\overset{*}{T}_i\} - \lambda_i[C]\{\overset{*}{T}_i\} = 0 \quad i = 1, 2, 3, \ldots, m \tag{4}$$

where λ_i is the ith eigenvalue and represents a thermal decay coefficient, and $\{\overset{*}{T}_i\}$ is the eigenvector corresponding to the ith eigenvalue. The eigenvectors are referred to as thermal mode shapes, analogous to vibration mode shapes from a free-vibration eigenvalue problem. In the first eigenvalue problem, the elements of $[K]$ and $[C]$ are evaluated for thermal properties corresponding to initial temperatures for the transient problem. In the second eigenvalue problem, the matrices are evaluated for thermal properties corresponding to temperatures obtained from the solution of a nonlinear steady-state problem with time-averaged thermal properties and heat loads from the transient problem. Only a subset of the eigenvectors is used, and selection of the eigenvectors to be retained is a crucial step in the reduction method, which is described in subsequent sections of this report.

The reduced system of equations is obtained by substitution of equation (2) into equation (1) and premultiplying both sides of the resulting equation by the transpose of $[\Gamma]$. A reduced system of equations in terms of the unknown generalized coefficients results, as follows:

$$[\overline{K}]\{\psi\} + [\overline{C}]\{\psi\} = \{\overline{Q}\} \tag{5}$$

where

$$\left.\begin{aligned} \underset{n,n}{[\overline{K}]} &= \underset{n,m}{[\Gamma]^T}\ \underset{m,m}{[K]}\ \underset{m,n}{[\Gamma]} \\ \underset{n,n}{[\overline{C}]} &= \underset{n,m}{[\Gamma]^T}\ \underset{m,m}{[C]}\ \underset{m,n}{[\Gamma]} \\ \underset{n}{\{\overline{Q}\}} &= \underset{n,m}{[\Gamma]^T}\ \underset{m}{\{Q\}} \end{aligned}\right\} \tag{6}$$

The barred quantities represent the reduced conductance and capacitance matrices and reduced heat load vector.

Implementation and Solution Technique

The SPAR finite-element thermal analyzer described in reference 14 was used to obtain solutions to the full system of equations (eq. (1)) for the transient heat transfer problems considered in this investigation. In the SPAR thermal analyzer, time- and temperature-dependent thermal properties in the conductance and capacitance matrices are treated by dividing the transient heat pulse into intervals (typically of 10- to 50-sec duration for problems considered herein) and reforming those matrices by assuming the time-dependent thermal properties have a constant value equal to the average value over the time interval. The temperature-dependent properties are evaluated for temperatures at the beginning of each time interval. For this investigation, equation (1) was numerically integrated over each time interval (for time-step sizes which ranged from 0.5 to 10 sec) by using the implicit Crank-Nicolson algorithm available in the SPAR thermal analyzer. This process is repeated continuously over the entire heat pulse to obtain the transient temperature response for any given problem. With the SPAR thermal analyzer, it is also possible to output the conductance and capacitance matrices and the thermal load vector at the beginning of each time interval. This capability was used to implement the reduction method.

The SPAR program was used to generate conductance and capacitance matrices for the previously described eigenvalue problems. A standard eigenvalue extraction routine available on the computer operating system at the Langley Research Center was then used to solve the thermal eigenvalue problems (eq. (4)) to obtain thermal mode shapes for use as reduced basis vectors. These vectors were then used as the transformation matrix $[\Gamma]$ in a pilot computer program which formed and solved the reduced system of equations for the unknown generalized coordinates $\{\psi\}$. Nodal temperatures were then calculated by equation (2). Solution techniques in the pilot program were patterned after those used in the SPAR program. Since the thermal properties change from one time interval to the next, SPAR was used to form and output the conductance and capacitance matrices and heat load vector at the beginning of each time interval for use by the pilot computer program. It should be noted that in the analysis of any problem, only two eigenvalue analyses were made to obtain reduced basis vectors to establish the transformation matrix $[\Gamma]$, which was then used over the entire heat pulse to obtain the reduced system of equations. This process obviously requires a large amount of computer input and output activity, which is usually inefficient; however, the intent of this investigation was to determine if substantial reductions in the number of degrees of freedom could be achieved for transient thermal problems by using the reduction method, and the use of a "brute force" approach was considered sufficient for such a determination. Results from the reduced system of equations were evaluated by comparison with results from the full system of equations from a SPAR analysis of each problem, as described in the next section. Time intervals and time steps used in the Crank-Nicolson integration algorithm within each time interval were the same for both the full and reduced systems of equations.

Thermal Problems and Results

To gain insight and experience with the reduction method for thermal analysis, the method has been applied to a series of increasingly complex problems. The initial problem consisted of calculating temperature histories in a portion of the Shuttle wing segment shown in figure 1 by using the reduction technique. The SPAR finite-element thermal model, shown in figure 2(a), represents a 58-in. segment of the lower surface of bay 3 and consists of a 0.119-in-thick aluminum sheet (to represent the structure) covered by a 1.36-in-thick layer of high-temperature reusable surface insulation (HRSI). The HRSI, strain isolator pad (SIP), and room temperature vulcanizing (RTV) adhesive were modeled with two-dimensional finite elements. One-dimensional elements with a quasi-linearized radiation representation (ref. 14) were used on the HRSI surface to model radiation losses, and one-dimensional conduction elements were used to model the aluminum structure. The grid shown has 84 node points and, hence, 84 degrees of freedom, since temperature is the only nodal degree of freedom. The lateral edges and backface were assumed to be adiabatic, and the surface was subjected to heat pulses similar to that shown in figure 2(b), which is reasonably representative of Shuttle reentry. Radiation from the surface and variation of the thermal properties of the HRSI cause the heat transfer equation to be nonlinear. Thermal properties (specific heat and conductivity) of the HRSI are functions of temperature and vary as indicated in figure 3. Further, because the HRSI is porous, the conductivity associated with air in the voids varies with pressure as well. Since the version of the SPAR thermal analyzer used in this study accommodates only temperature- and time-dependent properties, the pressure dependency was converted to a time dependency by utilizing the known pressure history for a typical Shuttle reentry trajectory.

To determine limitations on the reduction method, the spatial and temporal heating distributions for three problems shown in figure 4 were considered in this study. The spatial distribution is shown above the sketch of each model, and the temporal distribution is shown below. The first problem (fig. 4(a)) involved uniform heating on the surface of the 1.36-in-thick HRSI for a 2000-sec heat pulse. In the second problem (fig. 4(b)), the heating was symmetric over the surface. The thickness of the HRSI was reduced to 1 in. with an accompanying decrease in the heat pulse duration (to reduce computation times), so that temperatures reached values comparable to those for the uniform surface heating. In the third problem (fig. 4(c)), the heating was asymmetric over the HRSI surface. Since the surface heating in the first problem is uniform, it can be treated as a one-dimensional problem with essentially 14 degrees of freedom. The second

and third problems are treated as two-dimensional problems with essentially 42 and 84 degrees of freedom, respectively.

Uniform Surface Heating

Temperature distributions through the depth of the model with uniform surface heating computed with the full system of equations are shown in figure 5 for several discrete times during the heat pulse. The selected basis vectors must be able to accurately approximate these temperature distributions. Initially the entire structure is at a constant temperature of 560 °R. As heating is applied, the HRSI surface experiences a rapid temperature rise, which gradually diffuses through the HRSI and SIP to the aluminum skin. After peak heating occurs, the surface begins to cool while the interior of the HRSI and the aluminum skin continue to experience a temperature increase. The basis vectors must characterize this nonlinear response, give accurate solutions, and be easily and inexpensively generated. Nondimensional thermal mode shapes from a linear eigenvalue problem (in which matrices were evaluated at a uniform temperature of 560 °R) are shown in figure 6. Although numbered sequentially, these modes do not correspond to the five lowest eigenvalues from the eigenvalue problem associated with the two-dimensional finite-element model shown in figure 2. Because of the two-dimensional nature of the eigenvalue problem, most of the lower modes involved multiple waves in the lateral direction (y-direction in fig. 2(a)). Although 84 eigenvalues were extracted, only those modes with a single constant wave in the lateral direction are shown.

As indicated in reference 10, excellent correlation between the results from the reduced and full systems of equations was obtained with six basis vectors: modes 2 through 5 from figure 6; the reciprocal of the mode 1 vector, also shown in figure 6 (to enhance representation of the diffusion character of the transient temperature distribution), and a constant (unit) vector to accommodate uniform temperature changes. Results from the reduction method are compared with the full-system solution over the entire duration of the heat pulse in figure 7. Temperatures are shown for the surface, midpoint of the HRSI, and the aluminum structure. The reduction-method temperatures are within 2 °R of the full-system results for this 14-degree-of-freedom problem and indicate that for the uniform surface heating, six basis vectors give an excellent approximation to the full-system solution.

Symmetric Surface Heating

Since the set of eigenvectors from the eigenvalue problem based on the uniform initial temperature of 560 °R proved effective for the uniform heating problem, a similar set was tried for the same problem geometry but with a nonuniform symmetric distribution of the applied heating. However, since these vectors were constant in the lateral direction, they resulted in an erroneous temperature distribution, which only represented the average lateral temperature distribution from the full-system solution. To obtain results closer to the full-system solution, a set of basis vectors was generated from a second eigenvalue problem with thermal properties evaluated at temperatures obtained from a "pseudo" steady-state problem. In this pseudo steady-state problem, time-dependent thermal properties and heat input were averaged over the heat pulse, and temperatures in the aluminum were held at a value expected during the midportion of the heat pulse (685 °R). Only modes with a single wave in the lateral direction from this second eigenvalue problem were selected for use as basis vectors. In this instance, the single wave had a shape similar to the symmetric heating distribution. Sets of basis vectors which combined a constant (unit) vector with equal numbers of vectors from the first and second eigenvalue problems were used.

The average absolute error in nodal temperatures at $t = 300$ sec into the heat pulse as a function of the number of vectors used in the reduction method is shown in figure 8. Results presented in reference 10 indicated good agreement with full-system results over the entire heat pulse with 23 vectors. Since publication of reference 10, additional vectors have been used to approximate the temperature field for this problem. Eigenvectors based on initial temperature conditions were combined with eigenvectors based on temperatures from a steady-state problem with one-half the average heat input. Additionally, the reduction method has been refined to become an adaptive process by including the nondimensionalized temperature distribution from the previous time interval as a basis vector in the current time interval. (See the section on the reduction method for a description of the solution process.) The upper curve in figure 8 represents errors for the nonadaptive method, and the lower curve is for the adaptive method. For the symmetric heating problem, the adaptive method results in a converged solution with an average absolute error in nodal temperatures of 3.5 °R with only 13 basis vectors. Figure 9 shows a comparison between temperatures from the adaptive solution with 13 vectors and the full-system solution. Temperatures are shown for the surface, the midpoint of the HRSI, and the aluminum structure throughout the duration of the transient heat pulse. The agreement between the two solutions is very good and indicates that the reduction method, with about one-third the original number of degrees of freedom, can predict temperatures with reasonable accuracy for nonuniform symmetric heating.

Asymmetric Surface Heating

Since the combined set of basis vectors using thermal mode shapes from the initial and pseudo steady-state temperature eigenvalue problems gave reasonable approximations for the problem with symmetric surface heating, similar combined sets of basis vectors were tried for the problem with asymmetric surface heating. Although several different combinations of these vectors were tried, errors in the

nodal temperatures were as large as 200 °R. The vectors from the pseudo steady-state problem with a single wave in the lateral direction (y-direction, fig. 2(a)) contained large variations between maximum and minimum values in the lateral direction (up to a factor of 9 compared with the variation in surface heating of about a factor of 2). This variation seemed to preclude obtaining a good approximation to the full-system solution. However, use of a set of vectors which combined modes from the pseudo steady-state problem and edge-to-edge reflections (mirror images about the vertical centerline) of those modes resulted in a better approximation.

Results presented in reference 10 indicate that reasonable agreement between results from the reduced and full systems was obtained with nine basis vectors from the average heating eigenvalue problem and their edge-to-edge reflections. Since publication of reference 10, additional sets of basis vectors based on temperature distributions corresponding to steady-state heating levels less than the average trajectory heating have been used to approximate temperatures for the asymmetric heating problem. The steady-state heating level was repeatedly reduced by a factor of 2 until a set of basis vectors was obtained which significantly improved the accuracy of the reduction method. Figure 10 shows the average absolute error in nodal temperatures for sets of basis vectors based on average heating and for one-sixteenth the average heating. The adaptive process was employed for both sets of basis vectors. Use of the vectors based on lower heating reduced the number of vectors required for a converged solution to 16 and reduced the average nodal temperature error from 9 °R to about 5.5 °R. A comparison of the temperatures from the reduction method and the temperatures from the full-system solution is shown in figure 11. Temperatures are shown for points on the surface, the midpoint of the HRSI, and the aluminum structure. Agreement between the reduction-method and the full-system solutions is reasonably good throughout the temperature history, with the maximum error less than about 4 percent. Thus, for this 84-degree-of-freedom problem, the reduction method gives good results with about one-fifth the original degrees of freedom.

Single Bay of Shuttle Wing

To investigate the effectiveness of the reduction method for thermal analysis of a more realistic structure, the technique was used to analyze the thermal response of bay 3 of the Shuttle wing segment shown in figure 1. Details of previous analyses of this structure are given in references 11 and 12. A thermal model of the structure and thermal protection system for bay 3 and a finite-element representation of the thermal model are shown in figure 12. In figure 12(a), the stringer-stiffened and corrugated aluminum structures are represented by various effective thicknesses denoted h. Similar to the simpler problems the HRSI, FRSI (flexible reusable surface insulation), SIP, and RTV were modeled by two-dimensional elements. A quasi-linearized radiation representation was used on the HRSI and FRSI surfaces to model radiation losses (ref. 14), and one-dimensional conduction elements were used to model the aluminum structure. The grid shown in figure 12(b) has 122 nodal points and, hence, 122 degrees of freedom. The lateral edges and aluminum structure were assumed to be adiabatic, and the two outer surfaces were heated by the heat pulses shown in figure 13. The nature of the heat pulses for both surfaces is significantly more complex than those in the previous problems, in that the spatial distribution changes dramatically on the lower surface as air in the boundary layer over the wing undergoes transition from laminar to turbulent flow beginning at about 650 sec into the heat pulse. Both the distribution of material and the imposed heating result in an asymmetric thermal response for this problem.

Based on the results from the previous problem with asymmetric heating, basis vectors were generated by solving an eigenvalue problem with temperatures from a pseudo steady-state problem for one-tenth the average applied heating from the heat pulses shown in figure 13. Again, only thermal mode shapes with a single half wave in the lateral direction and their edge-to-edge reflections (mirror images about the vertical centerline) were selected as basis vectors. Although several combinations of these vectors were tried, errors in the nodal temperatures were unacceptable. When additional mode shapes from an eigenvalue problem based on initial temperatures were included as basis vectors, reasonably accurate results were achieved. A set of basis vectors which included an adaptive mode, six modes based on initial conditions, a unit mode, and a variable number of modes from the set based on one-tenth the average heating was used as a suitable set of basis vectors for this problem. Three representative vectors from this set are given in table I. The first typifies vectors which had nearly equal dominance in the two surfaces of the wing. The second and third vectors typify those that were dominant in the lower and upper surfaces, respectively. Most of the vectors in the set were associated with dominance in the lower surface. Since the two surfaces were connected by the relatively thin aluminum webs (fig. 12(a)) and internal radiation was neglected, the thermal coupling between the two surfaces was very small.

A reduction-method solution was attempted with various numbers of basis vectors, and the convergence at 300 sec is shown in figure 14. Use of 36 vectors gave a solution having a maximum temperature error of 65 °R. A comparison between the reduction-method and full-system results for $t = 300$ sec is shown in figure 15. The agreement between the two solutions is very good; however, when the solution was extended further into the heat pulse, the errors in the model temperatures from the reduction-method results increased to about 200 °R in the aluminum webs which connect the two wing surfaces. These large errors are believed to stem from the weak coupling between the two wing surfaces, which results in very few eigenvectors that are dominant in the aluminum web region of the structure. After several futile attempts to determine additional basis vectors

which would improve the results, solution of this problem was abandoned. It was hypothesized that for such weakly coupled problems, it may be beneficial to separate the problem into parts, each with its own set of basis vectors. This hypothesis is tested on a problem consisting of only the lower wing surface of bay 3, as described in the next section.

Lower Surface of Bay 3 of Shuttle Wing

The finite-element model (fig. 12(b)) was modified to retain only the lower aluminum skin and its associated thermal protection system on the lower surface of bay 3 of the Shuttle wing. The lateral edges and aluminum skin were assumed to be adiabatic, and the outer surface was assumed to be heated by the heat pulse for the lower wing surface (fig. 13(a)). Because of the material distribution and spatial variation of the heat pulse, the thermal response is asymmetric. A set of basis vectors consisting of an adaptive mode, a unit vector, and 12 modes and their edge-to-edge reflections (including the reciprocal of the mode 1 vector) from an eigenvalue problem based on temperatures from a pseudo steady-state problem with one-tenth the average applied heating was used. Maximum errors of up to 9 percent occurred at about 600 sec into the heat pulse. These errors were considered excessive, and a second solution was obtained with a similar set of basis vectors from an eigenvalue problem based on initial temperature conditions. The maximum errors decreased to about 7 percent. The maximum errors occurred along the lateral edges of the model, which are significantly affected by the presence of heat sinks associated with the additional structural material where the wing webs meet the surface structure. Comparison of the basis vectors for this problem with those from the problem with a constant skin thickness and an asymmetric heat pulse revealed a greater lateral variation in the basis vectors associated with the heat sinks. Accordingly, to reduce the lateral variation in the basis vectors, a set of basis vectors based on initial temperatures was generated, but with the aluminum thicknesses at the model edges reduced from 0.304 to 0.152 in. and from 0.289 to 0.145 in. The basis vector set consisted of an adaptive mode, a unit mode, and up to 12 modes and their edge-to-edge reflections (including the reciprocal of the mode 1 vector) from the eigenvalue solution for initial temperature and reduced aluminum heat sink thickness. A solution using 24 basis vectors from this set was found to have maximum errors of less than 5 percent, except from about 650 sec to 1100 sec into the heat pulse, when the maximum errors remained at the 7- to 8-percent level.

From figure 13, it is clear that the spatial distribution of the applied heating changes radically during the time interval from 650 to 1100 sec into the heat pulse. Figure 16 further illustrates these changes for various times between 650 and 1100 sec. Thus, to accommodate the changes in applied heating, it was necessary to add an analytically generated basis vector which incorporates the changing nature of the applied heating. An additional adaptive basis vector with the character of the applied heating at the model surface and a rapid decay rate in the model interior was generated as a function of position, as follows:

$$\Gamma(x_j, y_k) = e^{-20x_j/\ell}\ Y(y_k) \tag{7}$$

where $Y(y_k)$ are the heating distributions in figure 16, x_j is the nodal position in the HRSI measured from the heated surface, y_k is the corresponding nodal position along the heated surface, and ℓ is the thickness of the thermal protection system. When this analytically determined basis vector was combined with the set from the eigenvalue problem based on initial temperatures and reduced aluminum heat sink thicknesses, the reduction method gave acceptable temperature errors over the entire heat pulse.

The maximum error in the nodal temperatures is shown in figure 17 as a function of the number of basis vectors. Convergence was obtained with the 23 basis vectors listed in figure 17 at 200 sec into the heat pulse. The maximum error with these 23 basis vectors is shown in figure 18 for the entire heat pulse and indicates that inclusion of the vector of equation (7) reduced the maximum error to 4 percent or less. Temperatures from the reduction method using 23 basis vectors are compared with temperatures from the full system of equations in figure 19. Temperatures are shown for the HRSI surface, an interior point of the HRSI, and the aluminum structure for three lateral locations: the left side, the point of maximum temperature in the aluminum structure, and the right side. The reduction-method results agree reasonably well with those from the full system at each location over the entire heat pulse. Thus, for this reasonably complex 84-degree-of-freedom problem, the reduction method gives satisfactory results with about one-third the original degrees of freedom.

Large Space Antenna

The reduction method was applied to the thermal analysis of the reflector of a graphite/epoxy tetrahedral truss antenna associated with the microwave radiometer spacecraft (MRS) shown in figure 20. The MRS is designed to measure soil moisture from low Earth orbit and is described in reference 13. A 109-degree-of-freedom finite-element model of the reflector is shown in figure 21. The structure consists of two sets of surface elements joined by a set of diagonal elements and is modeled with one-dimensional tubular conduction and radiation elements. The temperature-dependent thermal emissivity ε and specific heat c_p for the graphite/epoxy composite are shown in figure 22. In this problem, heat transfer by conduction is essentially negligible relative to the radiation heat transfer (ref. 13); however, the thermal mass and specific heat are sufficient to require a transient analysis rather than steady-state solutions for accurate predictions of temperatures in the structure. The maximum and minimum heating rates for the surface elements and the

diagonal elements for a single orbit of the MRS are shown in figure 23.

In an initial solution attempt, a set of basis vectors for this problem was generated by solving an eigenvalue problem based on temperatures from steady-state heating at $t = 0$. A solution obtained with 20 of these basis vectors had maximum errors of 22 °R (nearly as large as the maximum temperature differences expected in the structure). Additional vectors improved the results, but the process was converging slowly, and it was apparent that a large number of basis vectors would be required for convergence. A second set of basis vectors was generated with five steady-state temperature distributions at the time slices indicated in figure 24 and a unit vector. Plots of absolute errors in nodal temperature for the two solutions are shown in figure 25 for a single orbit. Maximum errors for the second set of basis vectors were less than 3.5 °R. A comparison between the reduction method using the second set of basis vectors and the full-system solution for maximum and minimum temperatures in the antenna for a single orbit is shown in figure 26. Differences between the two solutions were only about 0.5 °R, so the two solutions are plotted as single curves. Thus, for this 109-degree-of-freedom radiation-dominated problem, accurate results were obtained by the reduction method for a problem size reduction of a factor of 18.

Concluding Remarks

A reduction method which combines classical Rayleigh-Ritz modal superposition techniques with contemporary finite-element methods to retain modeling versatility as the problem size (number of degrees of freedom) is reduced has been applied to transient nonlinear thermal analysis. The method has been used to obtain approximate solutions for temperature histories of models of a portion of the Shuttle orbiter wing subject to reentry heating and to a large space antenna reflector subject to heating associated with a low Earth orbit. Results were found to be highly dependent on the choice of basis vectors. Sets of eigenvectors obtained from two thermal eigenvalue problems associated with the transient problems were used as the initial choice of basis vectors in the approximate solutions. The first eigenvalue problem was based on thermal properties evaluated at the initial temperature conditions. The second was based on thermal properties evaluated for a temperature distribution corresponding to a nonlinear steady-state problem with time-averaged thermal properties and heating from the transient problem. Additionally, to achieve improved accuracy with fewer basis vectors, it was necessary to add an adaptive vector based on the temperature distribution from the previous time interval, a constant (unit) vector, the reciprocal of the first eigenvector, and reflections (mirror images) of the vectors from the eigensolutions. Good agreement was obtained between the reduction-method and full-system solutions for the conduction-dominated Shuttle wing problems with size reductions up to a factor of 5 for simplistic representations of the Shuttle wing structure (i.e., constant material distribution and spatially uniform heating). However, when more realistic representations of the structural and thermal protection system material distributions and spatially varying heating were considered, it was necessary to enrich the set of basis vectors. By adding an analytically generated vector based on the changing heat distribution, maximum temperature errors were reduced to 4 percent for problem size reductions of a factor of 3.

For the radiation-dominated orbiting large space antenna, the reduction method was found to give unacceptable temperature errors when thermal eigenvectors were used as basis vectors. However, when temperature distributions corresponding to steady-state temperature distributions at several time slices in the orbital heating profile were used as basis vectors, maximum temperature errors of less than 3.5 °R were achieved for the entire orbit while achieving a problem size reduction of a factor of 18.

The results of this paper indicate that the reduction method has excellent potential for significant size reduction for radiation-dominated problems. For conduction-dominated problems, the large reductions in problem size accrued only for those with the simplest geometry and heating distributions. For more complex conduction-dominated problems, especially those with complex spatial and temporal variations in the applied heating, additional work was necessary to generate alternate basis vectors which permit significant problem size reductions.

Langley Research Center
National Aeronautics and Space Administration
Hampton, VA 23665
September 13, 1984

References

1. Noor, Ahmed K.: Recent Advances in Reduction Methods for Nonlinear Problems. *Comput. & Struct.*, vol. 13, no. 1-3, June 1981, pp. 31-44.

2. Bathe, Klaus-Jurgen; and Gracewski, Sheryl: On Nonlinear Dynamic Analysis Using Substructuring and Mode Superposition. *Comput. & Struct.*, vol. 13, no. 5-6, Oct.-Dec. 1981, pp. 699-707.

3. Knight, Norman F., Jr.: Nonlinear Structural Dynamics Analysis Using a Modified Modal Method. *A Collection of Technical Papers —AIAA/ASME/ASCE/AHS 24th Structures, Structural Dynamics and Materials Conference, Part 2*, May 1983, pp. 111-128. (Available as AIAA-83-0824.)

4. Noor, Ahmed K.; Balch, Chad D.; and Shibut, Macon A.: *Reduction Methods for Nonlinear Steady-State Thermal Analysis.* NASA TP-2098, 1983.

5. Noor, Ahmed K.; and Balch, Chad D.: *Hybrid Perturbation/Bubnov-Galerkin Technique for Nonlinear Thermal Analysis.* NASA TP-2145, 1983.

6. Rathjen, Kenneth A.: *CAVE: A Computer Code for Two-Dimensional Transient Heating Analysis of Conceptual Thermal Protection Systems for Hypersonic Vehicles.* NASA CR-2897, 1977.

7. Frisch, Harold P.: Thermally Induced Response of Flexible Structures: A Method for Analysis. *J. Guid. & Control*, vol. 3, no. 1, Jan.-Feb. 1980, pp. 92-94.

8. Jones, G. K.; Skladany, J. T.; and Young, J. P.: Role of IAC in Large Space Systems Thermal Analysis. *Computational Aspects of Heat Transfer in Structures*, NASA CP-2216, 1982, pp. 253-270.

9. Shore, Charles P.: Status Report on Development of a Reduced Basis Technique for Transient Thermal Analysis. *Computational Aspects of Heat Transfer in Structures*, NASA CP-2216, 1982, pp. 133-146.

10. Shore, Charles P.: Application of the Reduced Basis Method to Nonlinear Transient Thermal Analysis. *Research in Structural and Solid Mechanics — 1982*, NASA CP-2245, 1982, pp. 49-65.

11. Adelman, Howard M.; Haftka, Raphael T.; and Robinson, James C.: *Studies of Implicit and Explicit Solution Techniques in Transient Thermal Analysis of Structures.* NASA TP-2038, 1982.

12. Ko, William L.; Quinn, Robert D.; Gong, Leslie; Schuster, Lawrence S.; and Gonzales, David: Reentry Heat Transfer Analysis of the Space Shuttle Orbiter. *Computational Aspects of Heat Transfer in Structures*, NASA CP-2216, 1982, pp. 295-325.

13. Garrett, L. Bernard: *Interactive Design and Analysis of Future Large Spacecraft Concepts.* NASA TP-1937, 1981.

14. Marlowe, M. B.; Moore, R. A.; and Whetstone, W. D.: *SPAR Thermal Analysis Processors Reference Manual, System Level 16.* NASA CR-159162, 1979.

TABLE I. THERMAL MODE SHAPES FOR SHUTTLE WING SINGLE-BAY PROBLEM

[Table corresponds to finite-element model shown in fig. 12(b)]

(a) Equally dominant in upper and lower wing surfaces

−0.437	−0.568	−1.000	−0.983	−0.561	−0.466
−0.335	−0.373	−0.760	−0.744	−0.370	−0.330
−0.260	−0.278	−0.615	−0.600	−0.277	−0.257
−0.212	−0.223	−0.517	−0.504	−0.222	−0.211
−0.212	−0.223	−0.517	−0.503	−0.221	−0.211
−0.196					−0.195
−0.054					−0.063
−0.035					−0.040
−0.030					−0.032
−0.030	−0.030	−0.031	−0.032	−0.032	−0.032
−0.030	−0.030	−0.031	−0.032	−0.032	−0.032
−0.032	−0.032	−0.034	−0.035	−0.035	−0.035
−0.032	−0.032	−0.034	−0.035	−0.035	−0.035
−0.036	−0.036	−0.038	−0.039	−0.040	−0.039
−0.040	−0.041	−0.043	−0.043	−0.045	−0.045
−0.046	−0.046	−0.049	−0.050	−0.051	−0.051
−0.053	−0.054	−0.057	−0.058	−0.059	−0.059
−0.063	−0.065	−0.068	−0.069	−0.071	−0.071
−0.077	−0.080	−0.084	−0.085	−0.087	−0.087
−0.100	−0.103	−0.109	−0.110	−0.113	−0.113
−0.140	−0.146	−0.153	−0.156	−0.160	−0.160
−0.236	−0.246	−0.257	−0.261	−0.267	−0.267
−0.705	−0.738	−0.756	−0.766	−0.770	−0.773

(b) Dominant in lower wing surface

0	0	0	0	0	0
0	0	0	0	0	0
0	0	0	0	0	0
0	0	0	0	0	0
0	0	0	0	0	0
0					0
0					0
−0.003					−0.009
−0.076					−0.139
−0.049	−0.018	−0.056	−0.071	−0.033	−0.081
−0.046	−0.016	−0.053	−0.067	−0.028	−0.076
0.521	0.482	0.575	0.752	0.853	0.998
0.522	0.483	0.576	0.754	0.854	1.000
0.390	0.424	0.507	0.615	0.657	0.779
0.019	0.126	0.137	0.118	0.106	0.109
−0.318	−0.236	−0.304	−0.423	−0.476	−0.591
−0.416	−0.459	−0.552	−0.691	−0.772	−0.915
−0.260	−0.417	−0.471	−0.554	−0.631	−0.705
−0.006	−0.135	−0.123	−0.118	−0.146	−0.124
0.216	0.226	0.280	0.359	0.408	0.489
0.294	0.459	0.516	0.628	0.730	0.819
0.247	0.431	0.470	0.564	0.659	0.724
0.111	0.165	0.182	0.217	0.247	0.275

(c) Dominant in upper wing surface

0	0	0	0	0	0
0	0	0	0	0	0
0.019	0.020	0.020	0.020	0.020	0.020
−0.895	−0.956	−0.980	−1.000	−0.999	−0.956
0.010	0.026	0.031	0.030	0.026	0.009
0					0
0					0
0					0
0					0
0	0	0	0	0	0
0	0	0	0	0	0
0	0	0	0	0	0
0	0	0	0	0	0
0	0	0	0	0	0
0	0	0	0	0	0
0	0	0	0	0	0
0	0	0	0	0	0
0	0	0	0	0	0
0	0	0	0	0	0
0	0	0	0	0	0
0	0	0	0	0	0
0	0	0	0	0	0
0	0	0	0	0	0

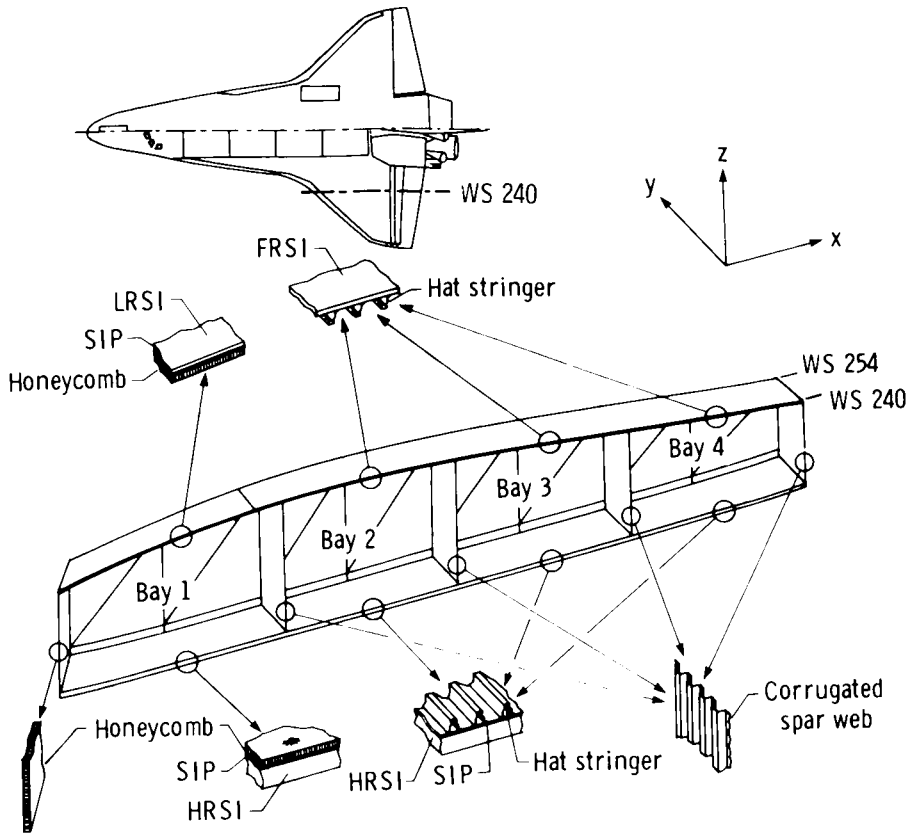

Figure 1. Geometry of Shuttle orbiter wing at WS 240.

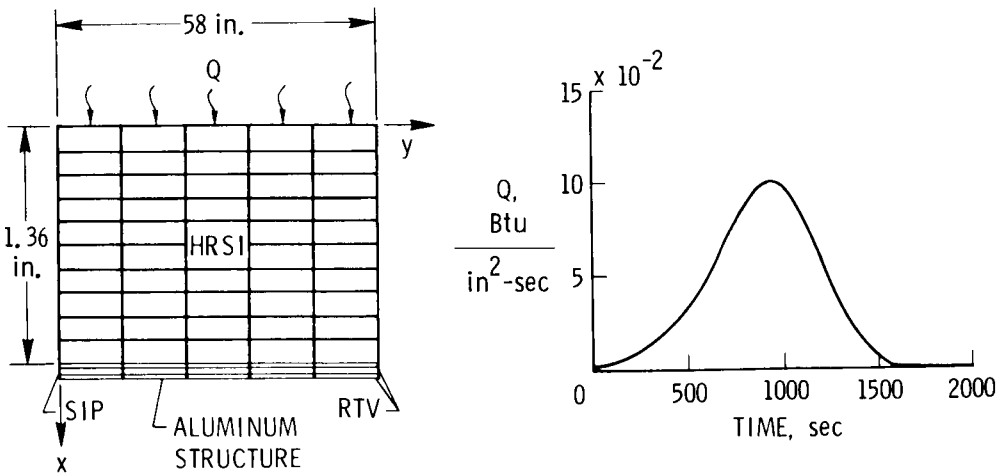

(a) Two-dimensional finite-element model (not to scale).

(b) Heat pulse.

Figure 2. Simplified model of Shuttle orbiter wing.

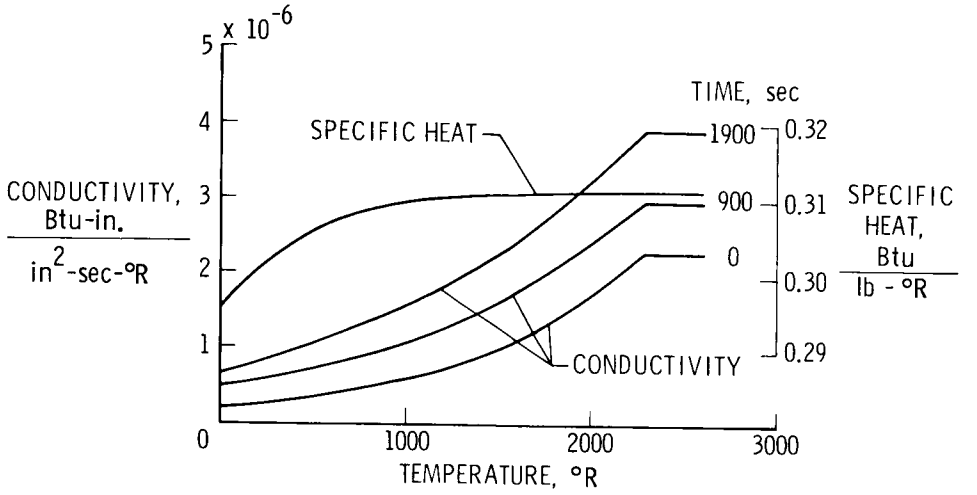

Figure 3. HRSI thermal properties.

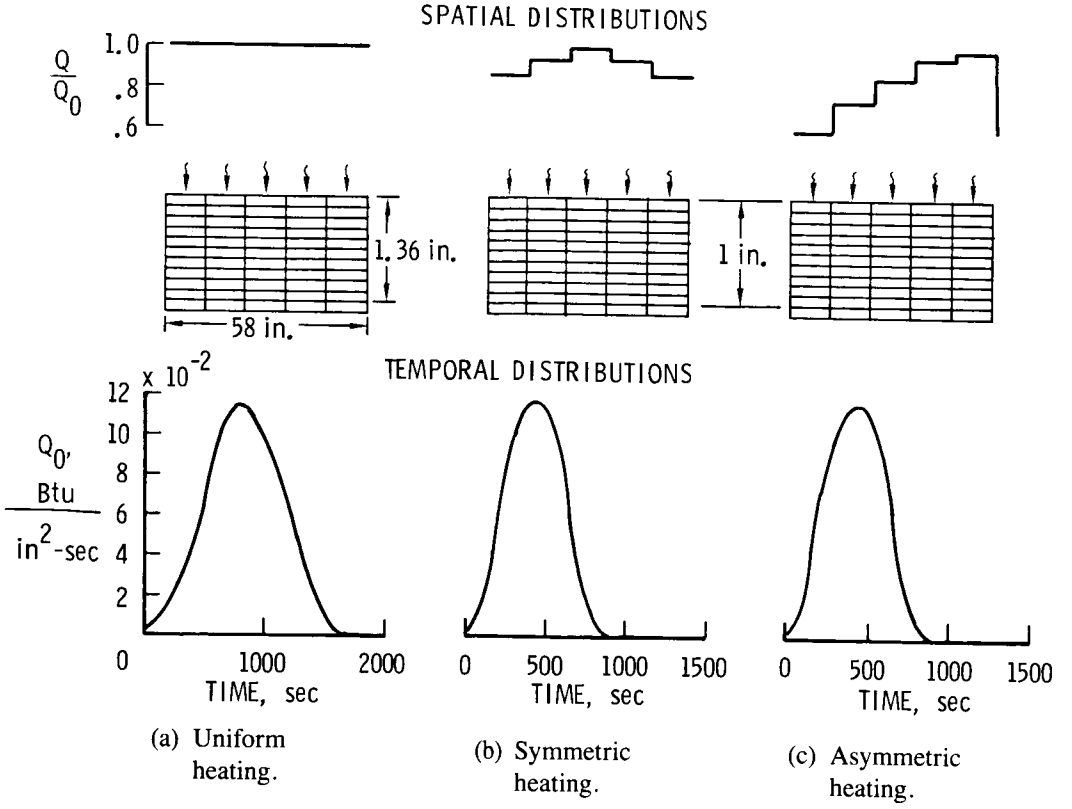

(a) Uniform heating.

(b) Symmetric heating.

(c) Asymmetric heating.

Figure 4. Heating distributions for sample problems.

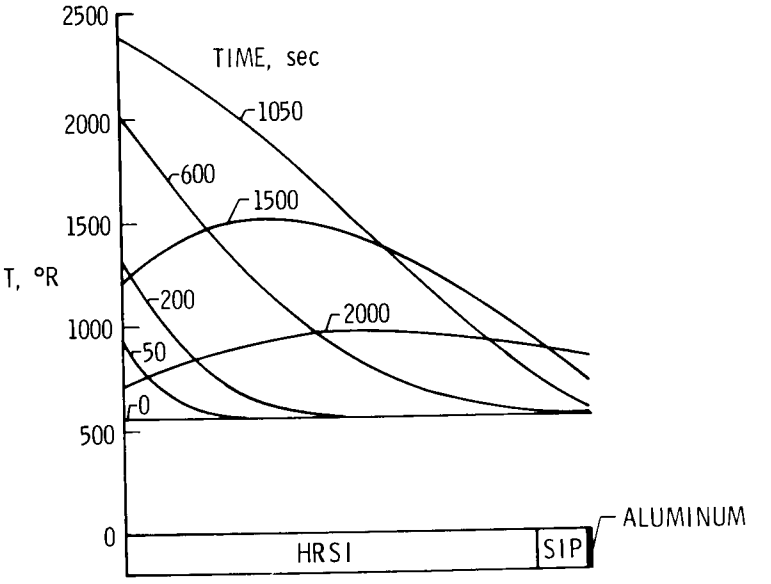

Figure 5. Temperature distributions for problem with uniform heating.

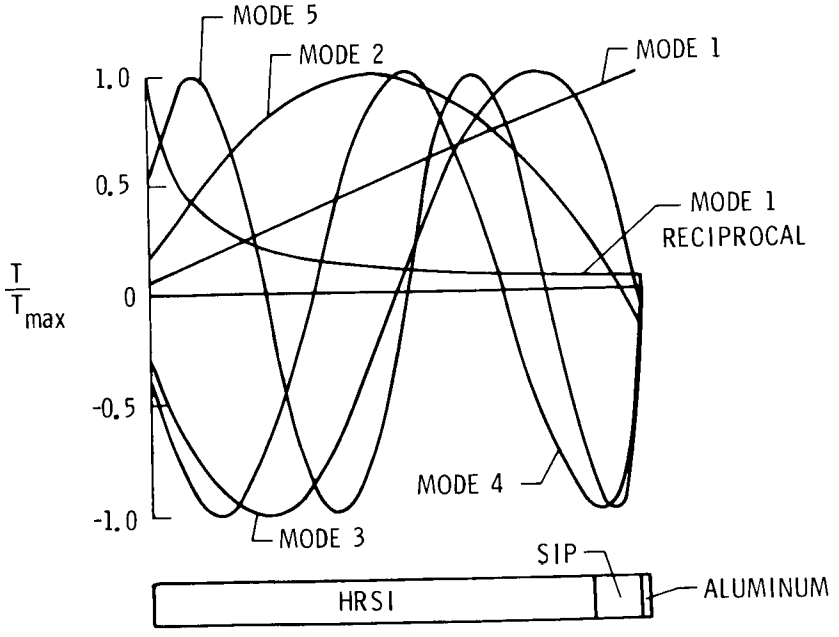

Figure 6. Thermal mode shapes for problem with uniform heating.

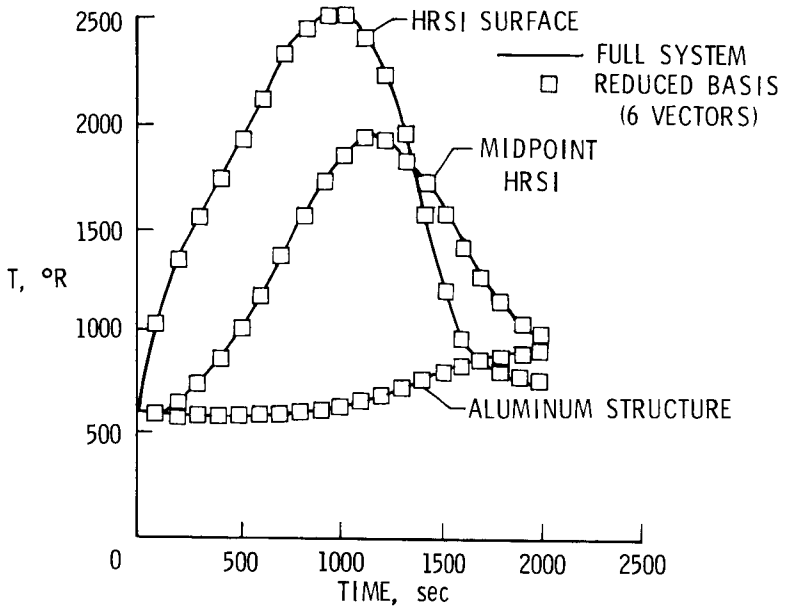

Figure 7. Comparison of reduced-basis and full-system temperatures for simplified wing with uniform heating.

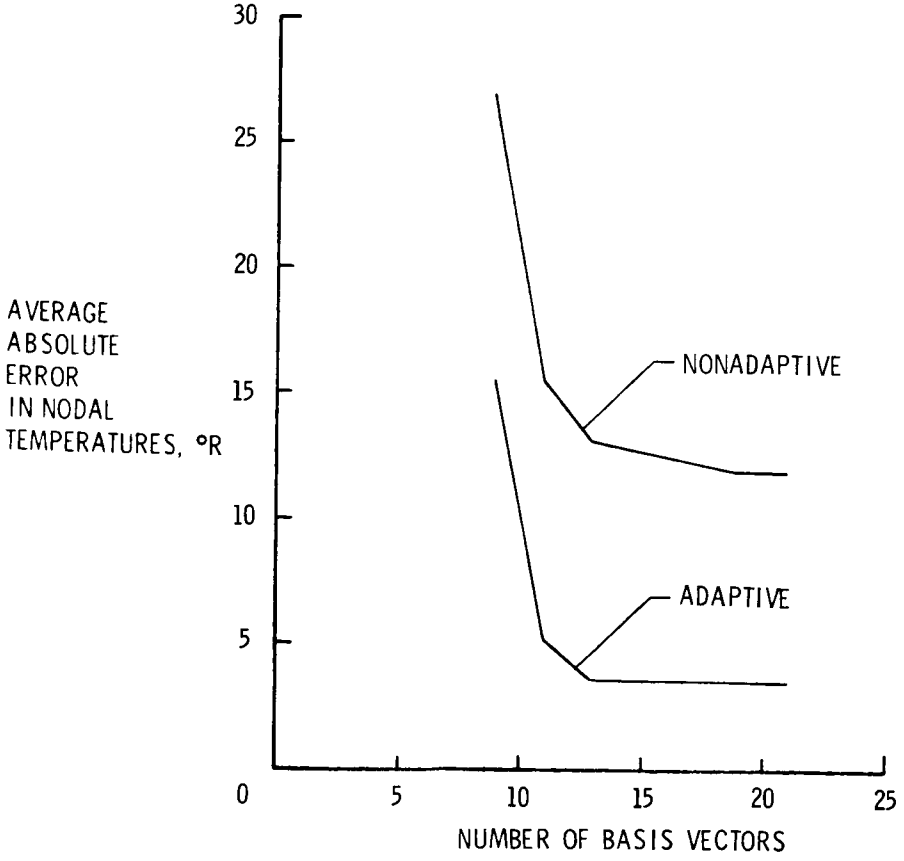

Figure 8. Convergence of adaptive reduction method for simplified wing with symmetric heating. t = 300 sec.

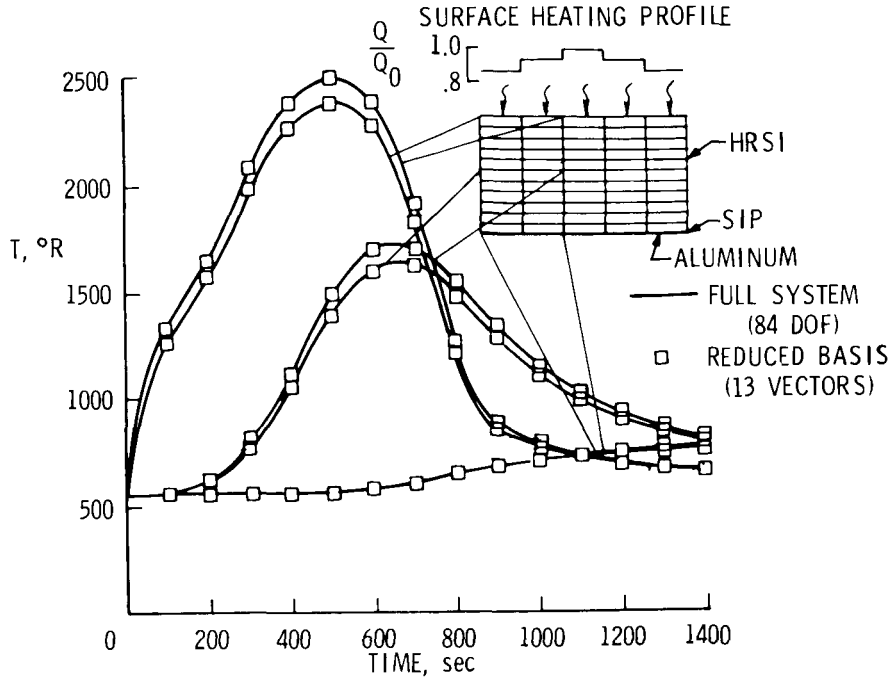

Figure 9. Comparison of reduction-method and full-system temperatures for simplified wing with symmetric heating.

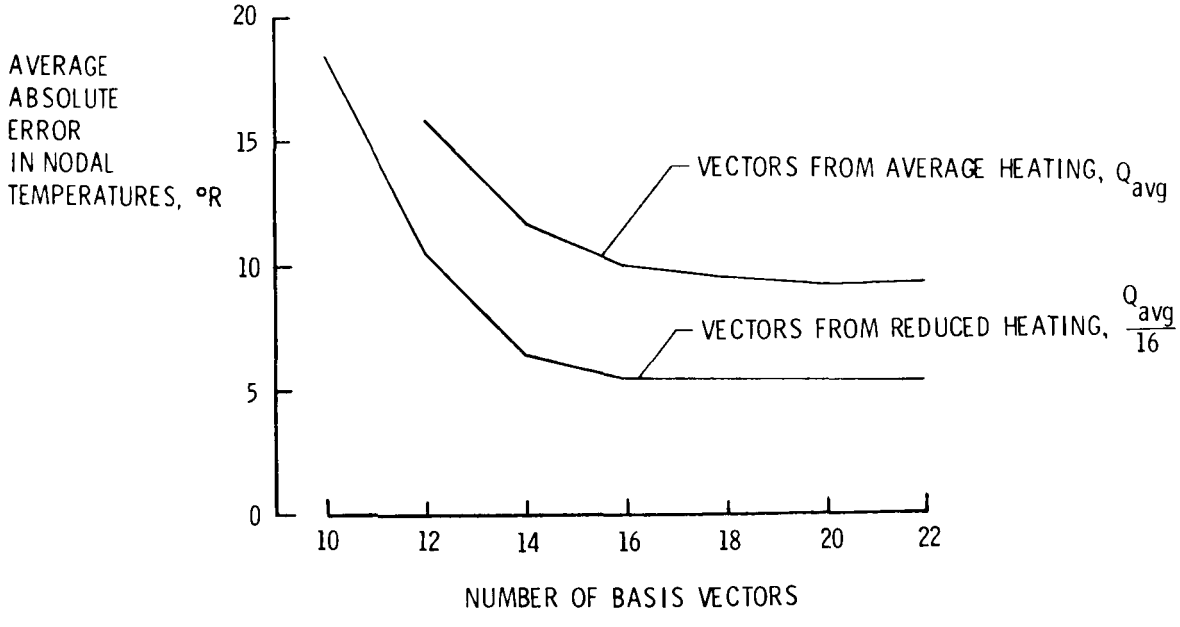

Figure 10. Convergence of reduction method using vectors from reduced heating for simplified wing with asymmetric heating. t = 300 sec.

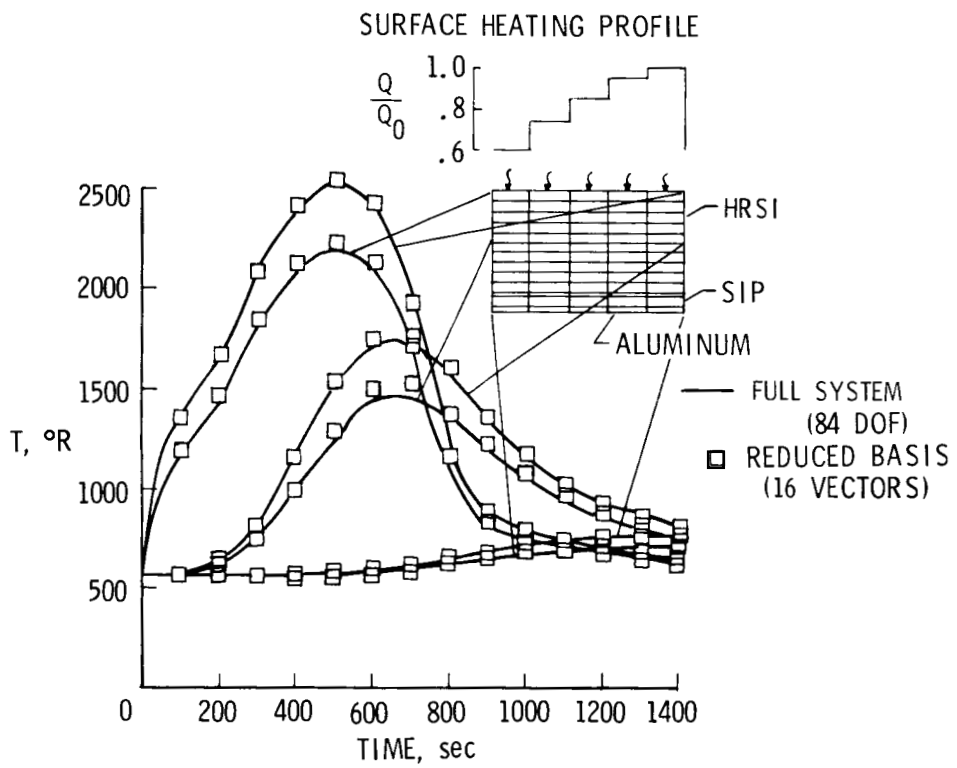

Figure 11. Comparison of reduction-method and full-system temperatures for simplified wing with asymmetric heating.

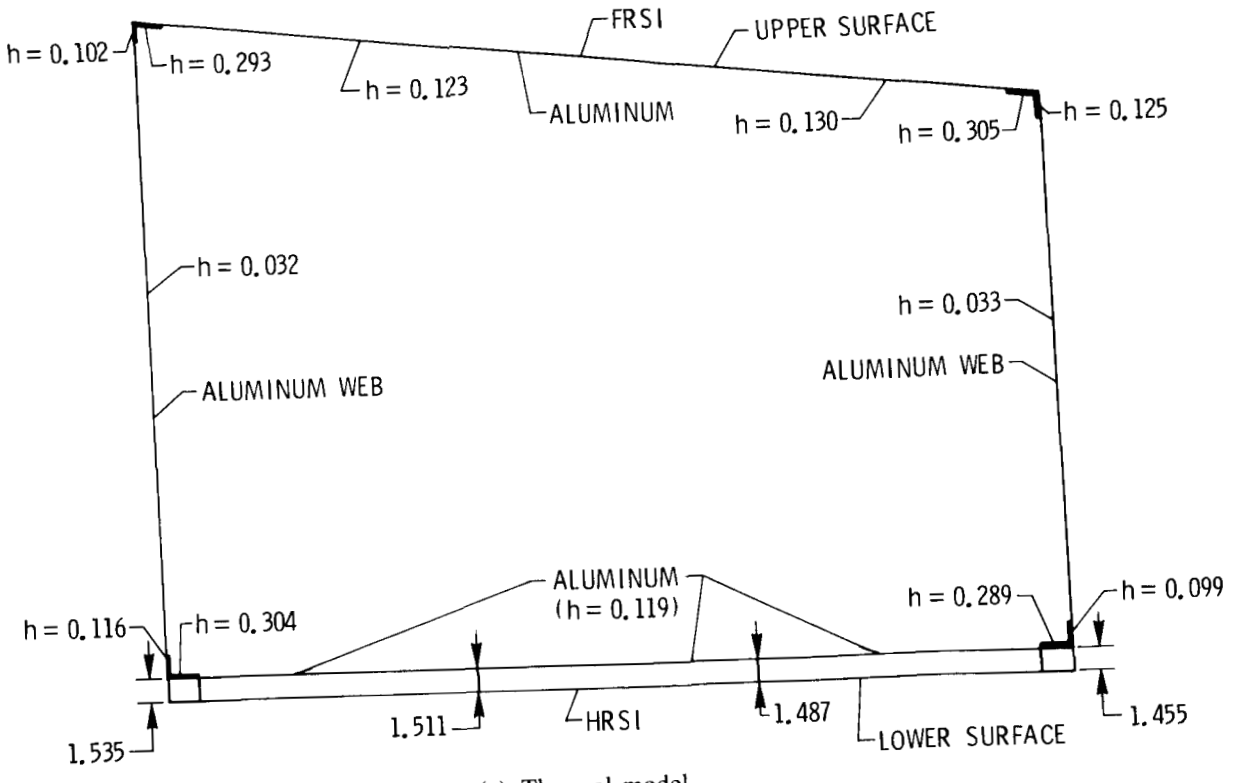

(a) Thermal model.

Figure 12. Model of bay 3 of Shuttle wing. All dimensions in inches.

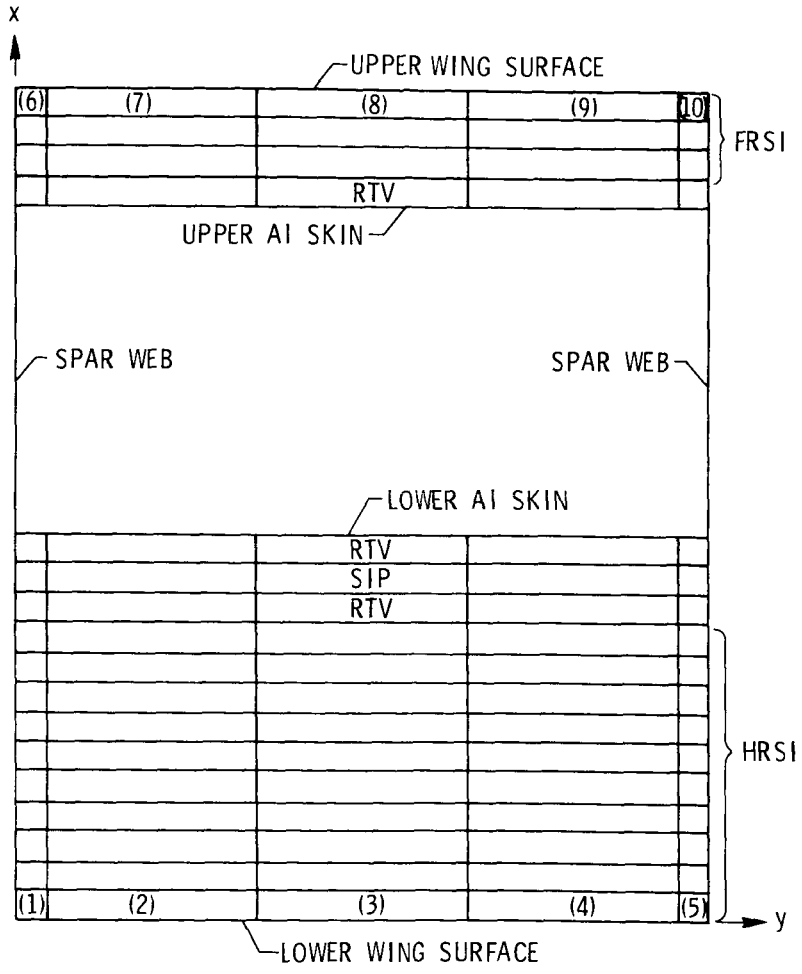

(b) Finite-element model (122 DOF). Numbers in parentheses denote heated surface elements.

Figure 12. Concluded.

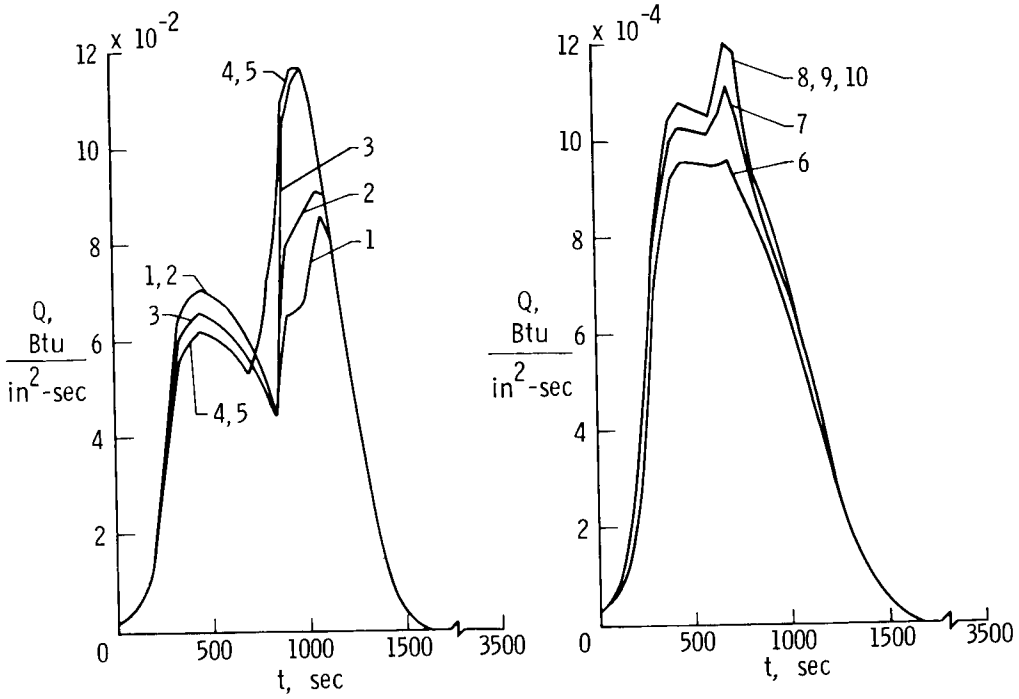

(a) Lower surface.

(b) Upper surface.

Figure 13. Heat pulse for bay 3 of Shuttle wing. Numbers refer to element numbers in figure 12(b).

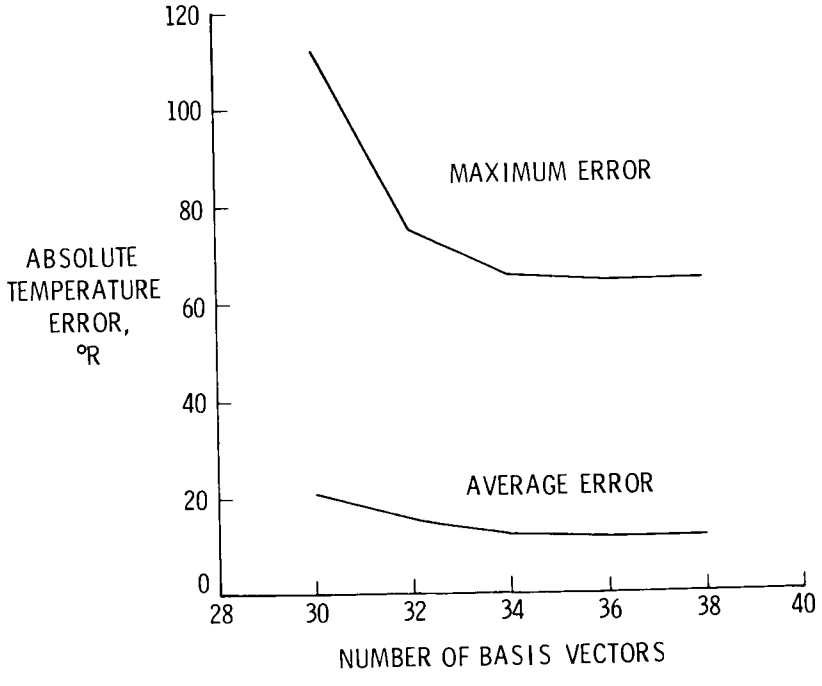

Figure 14. Convergence using modes based on initial conditions and one-tenth average heating for bay 3 of Shuttle wing. t = 300 sec.

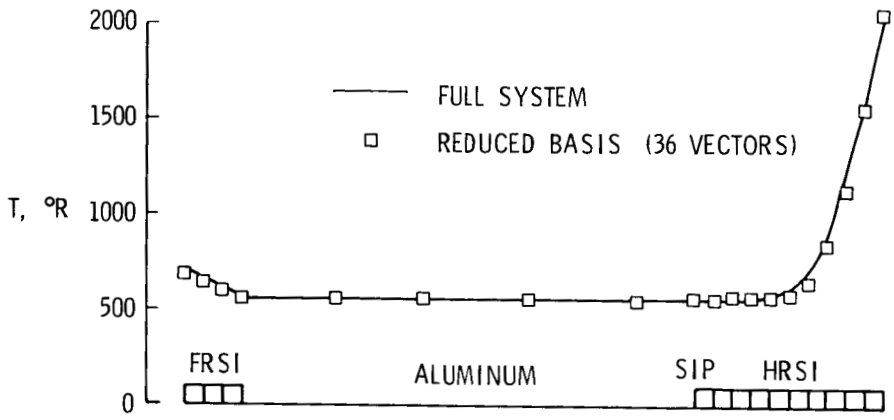

Figure 15. Comparison of reduction-method and full-system temperatures for bay 3 of Shuttle wing at t = 300 sec (122 DOF).

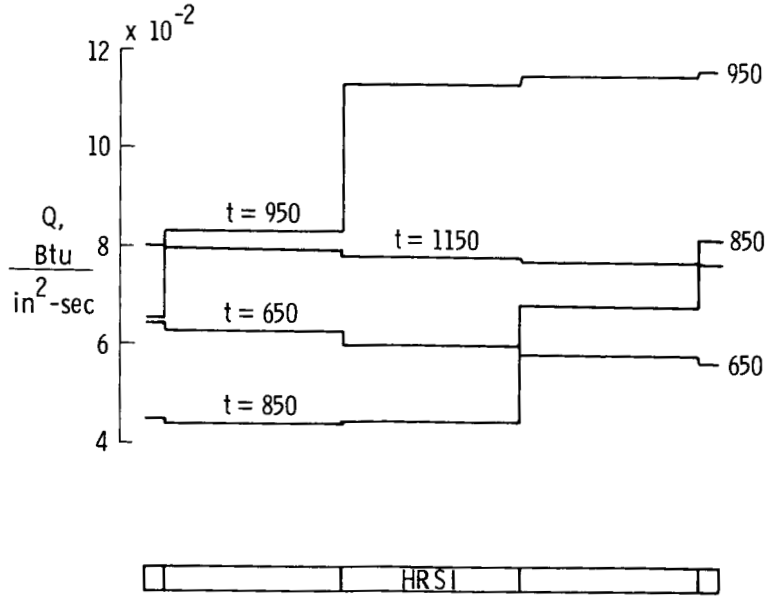

Figure 16. Spatial changes in lower surface heating for single-bay problem. t = 650 to 1150 sec.

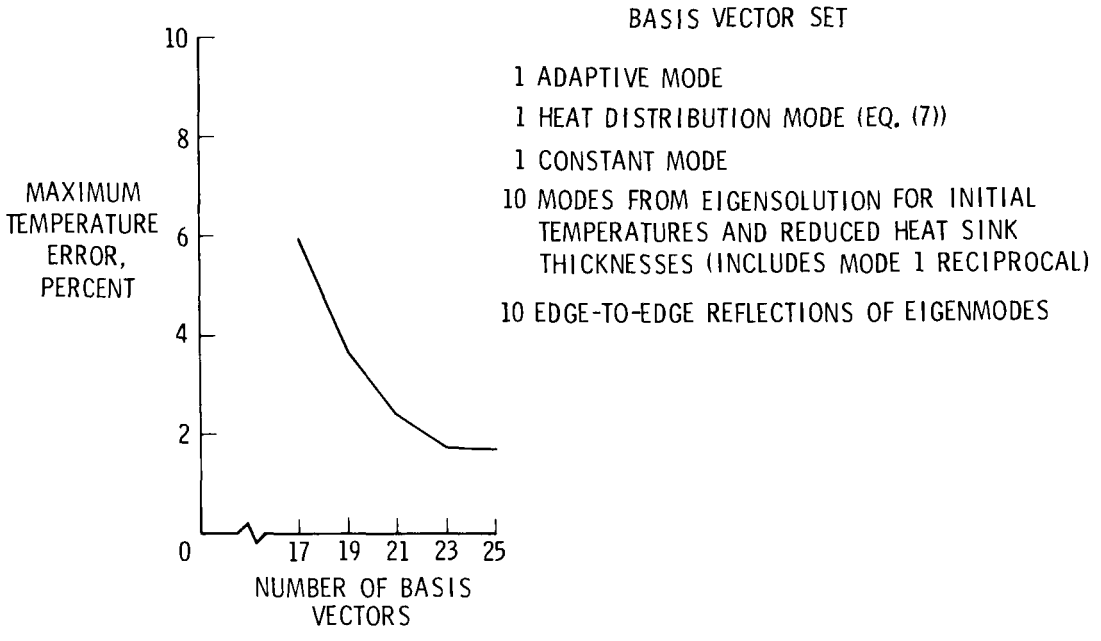

Figure 17. Convergence for lower surface of bay 3.

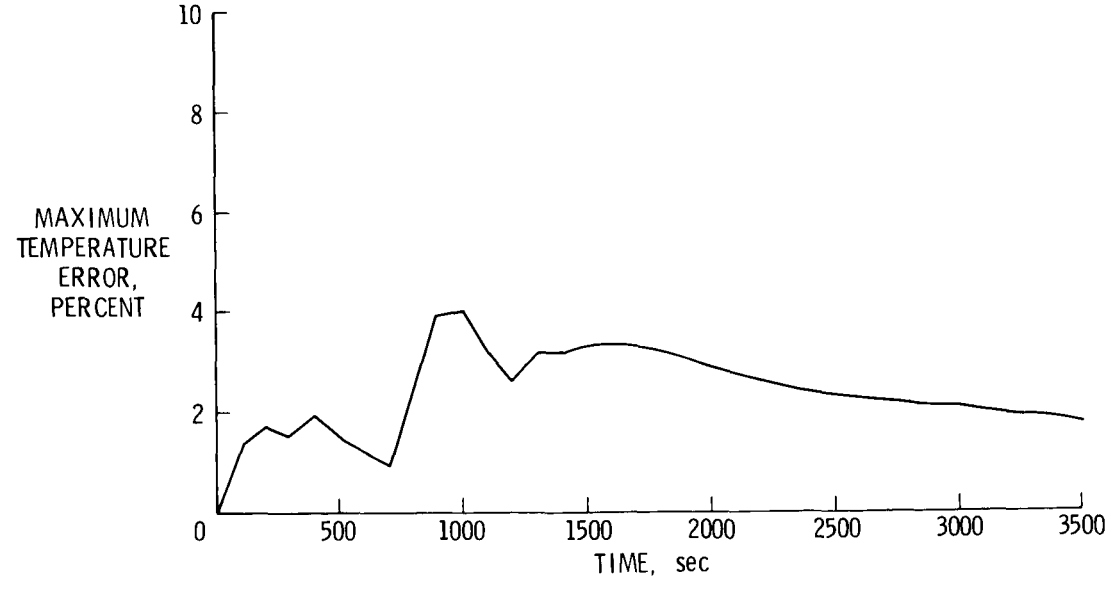

Figure 18. Maximum percent error for Shuttle wing segment, bay 3, lower surface problem. Twenty-three basis vectors.

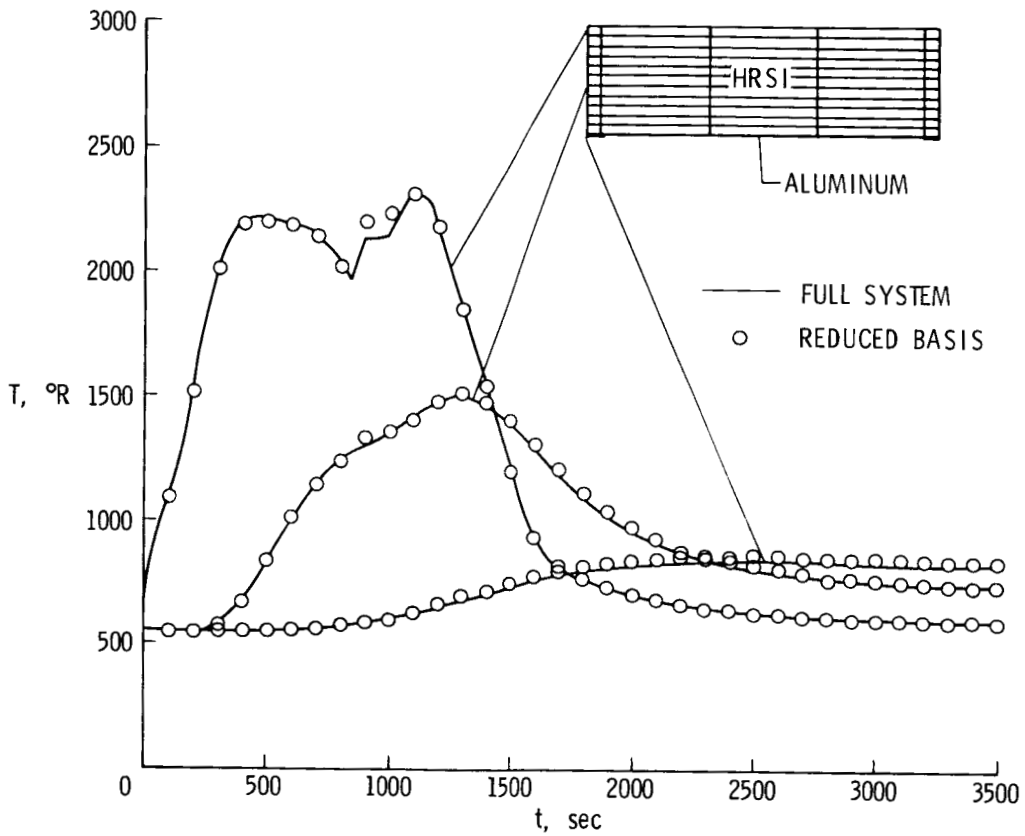

(a) Left side.

Figure 19. Comparison of reduction-method and full-system temperatures for Shuttle wing segment, bay 3, lower surface.

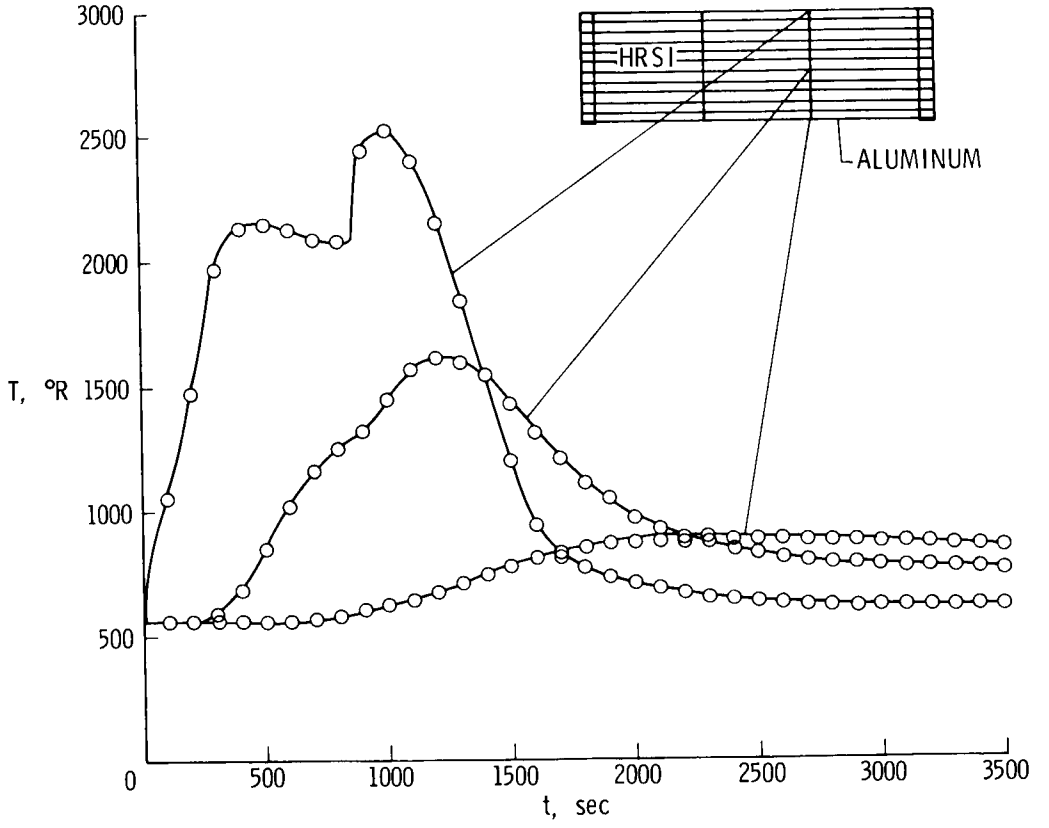

(b) Location of maximum temperature in aluminum structure.

Figure 19. Continued.

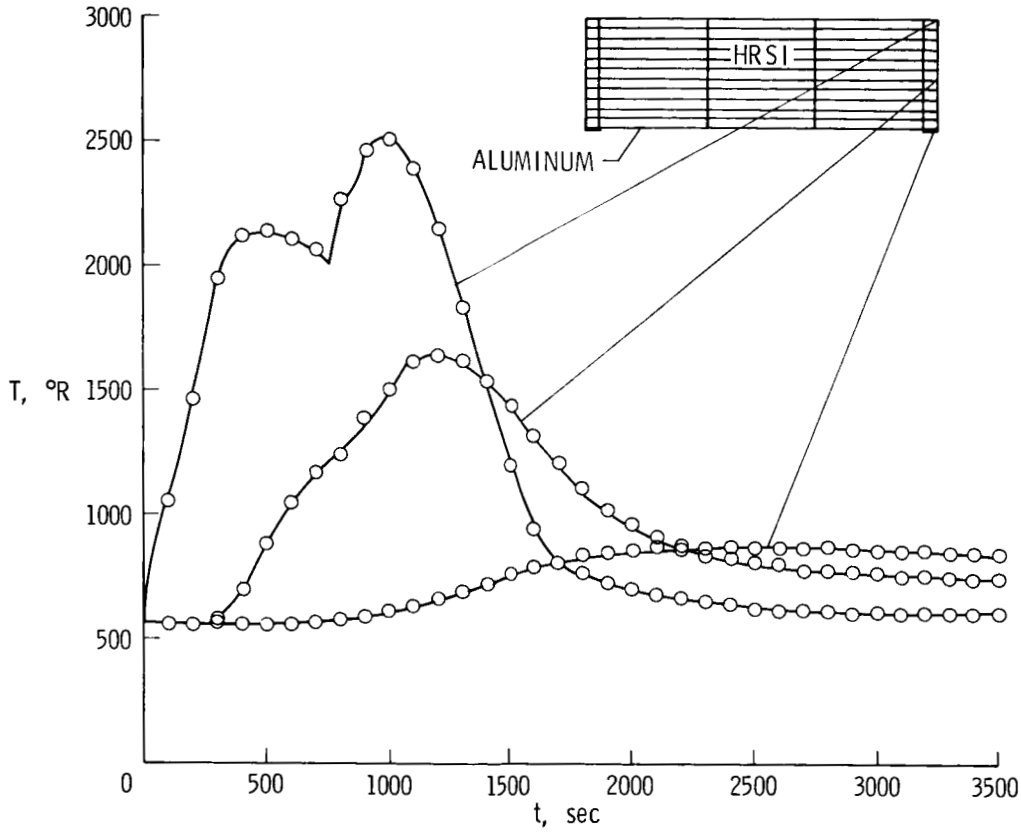

(c) Right side.

Figure 19. Concluded.

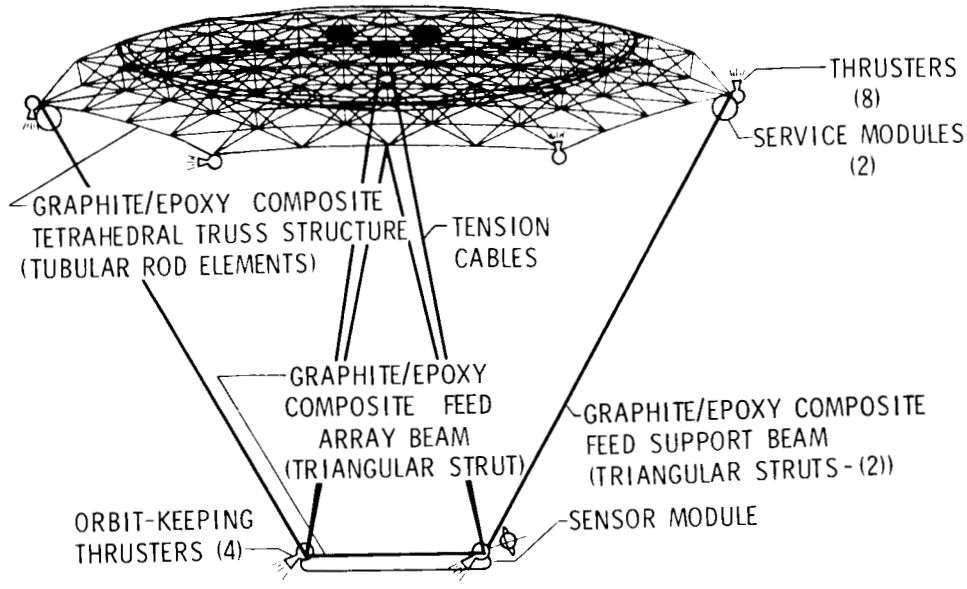

Figure 20. Microwave radiometer spacecraft (from ref. 13).

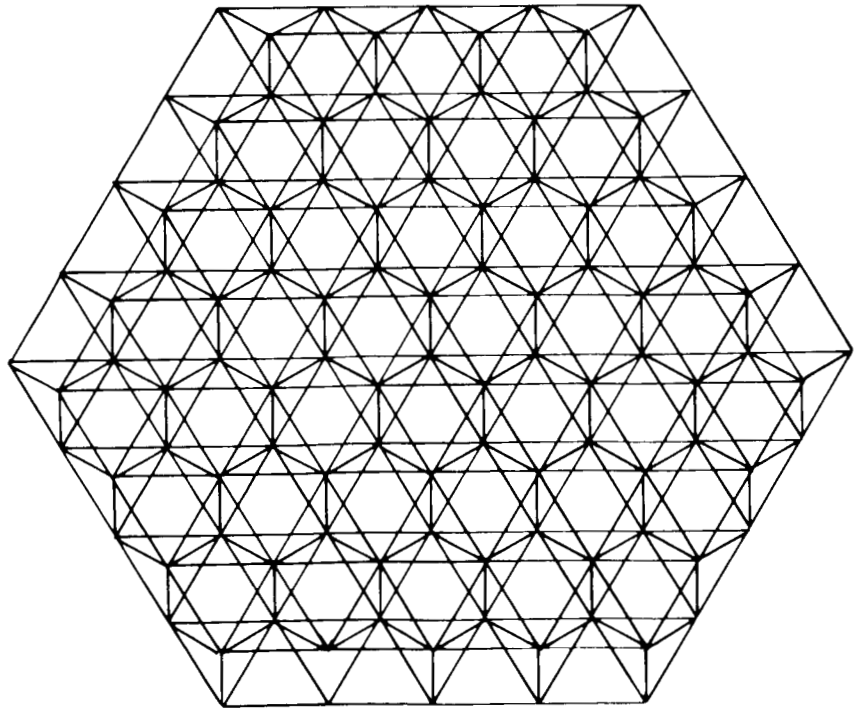

Figure 21. Finite-element model of antenna reflector (109 DOF).

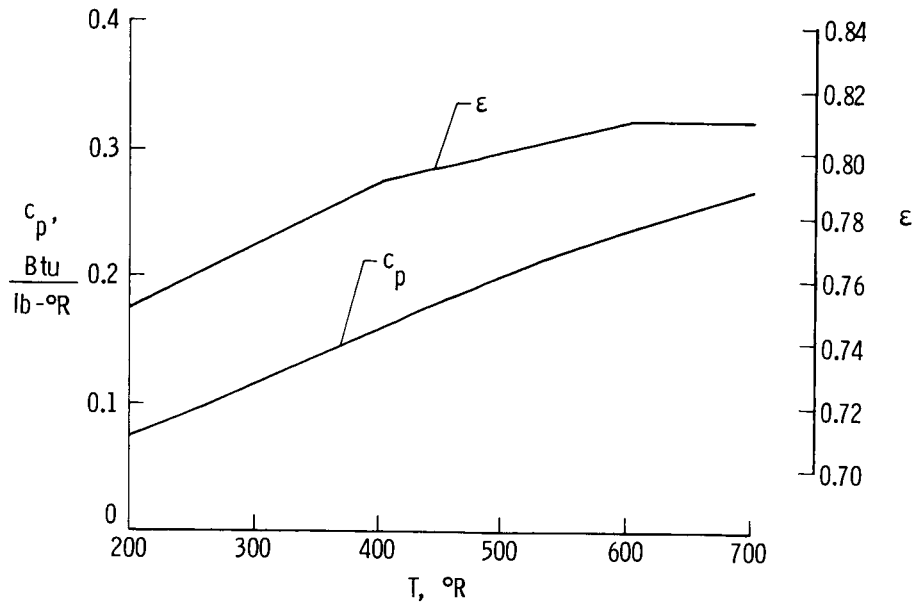

Figure 22. Thermal properties of graphite/epoxy antenna reflector.

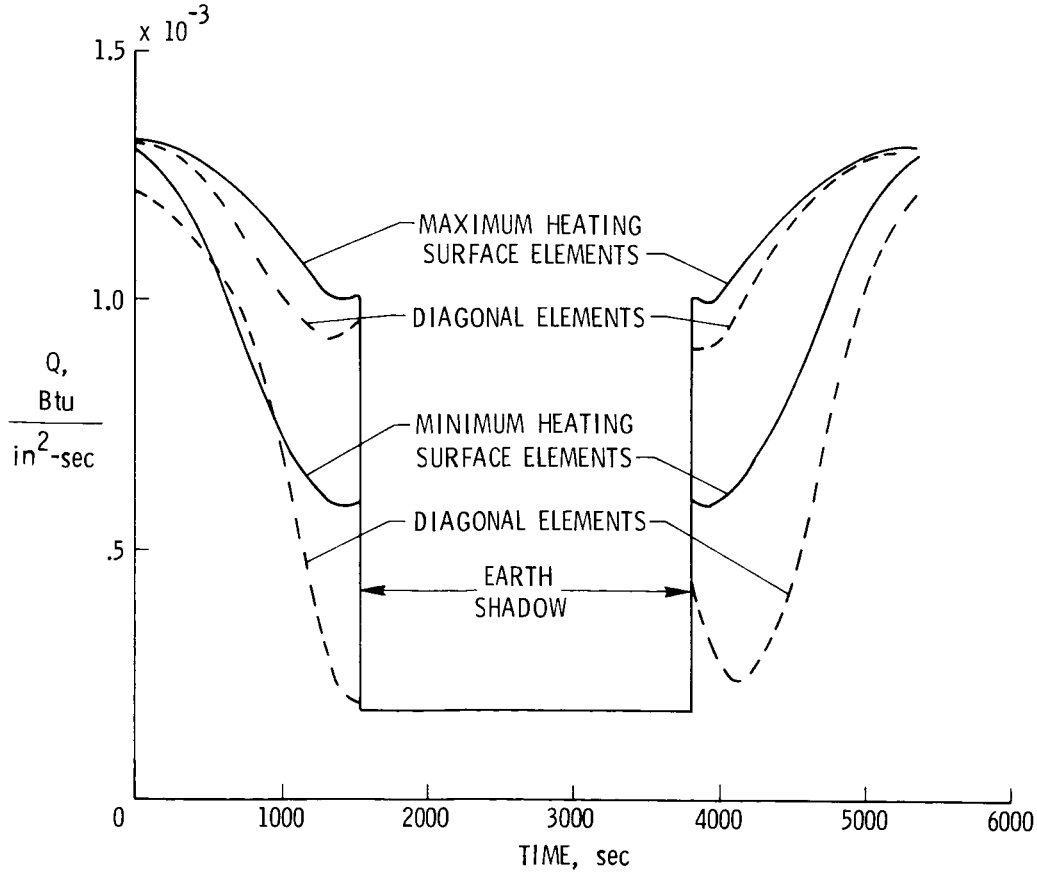

Figure 23. Orbital heating for antenna reflector.

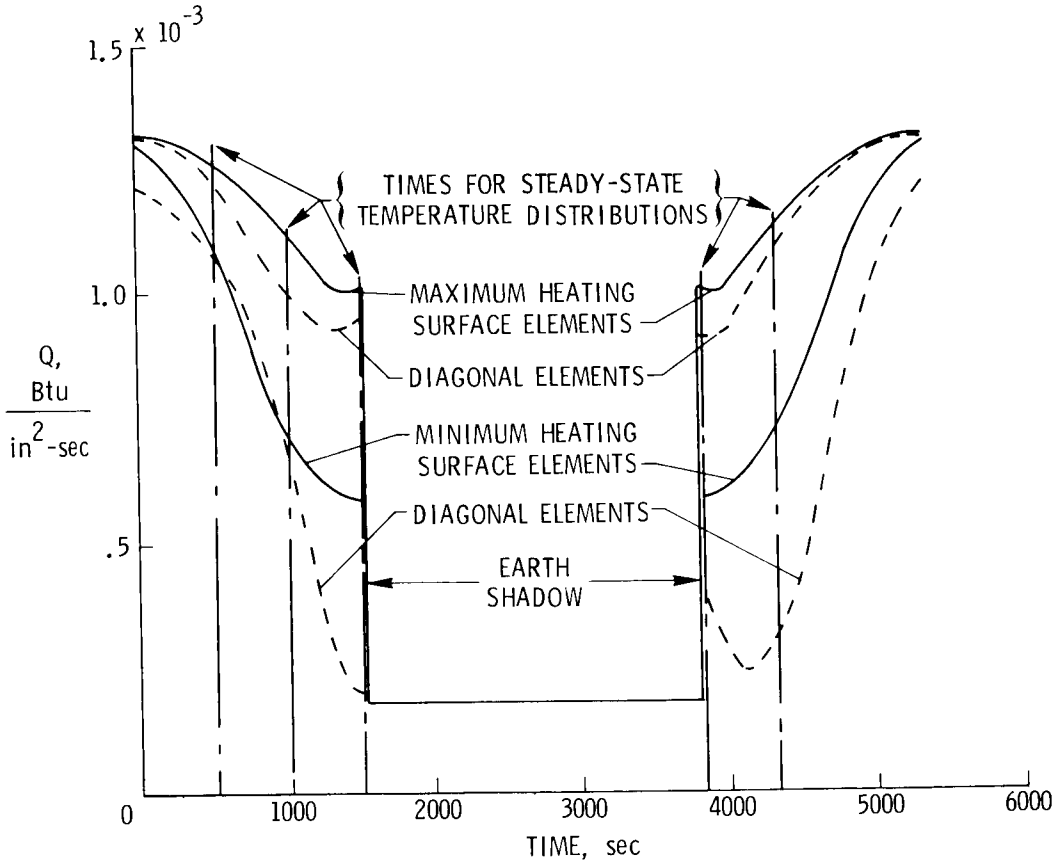

Figure 24. Times for steady-state temperature distributions used as basis vectors.

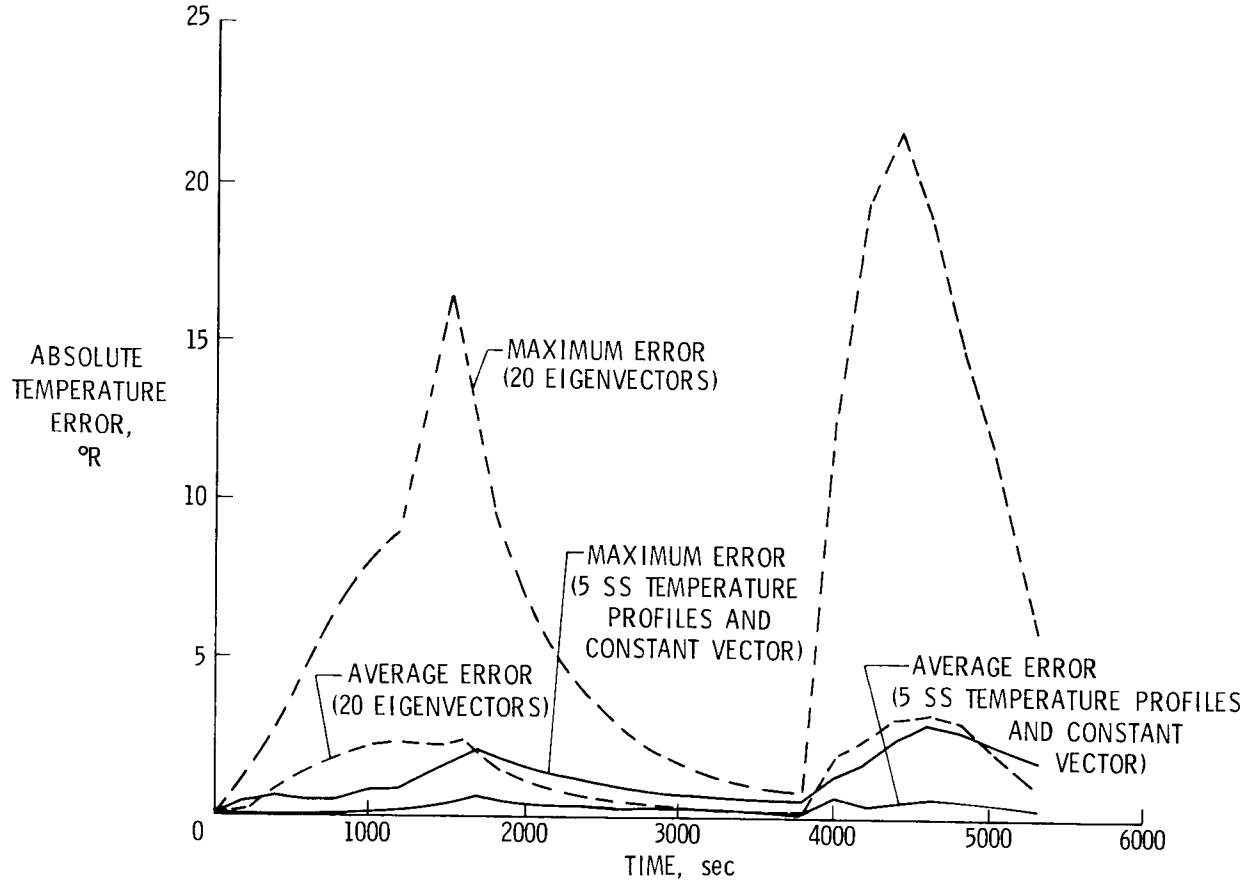

Figure 25. Comparison of temperature errors for antenna reflector (eigenvectors versus steady-state (SS) temperature profiles).

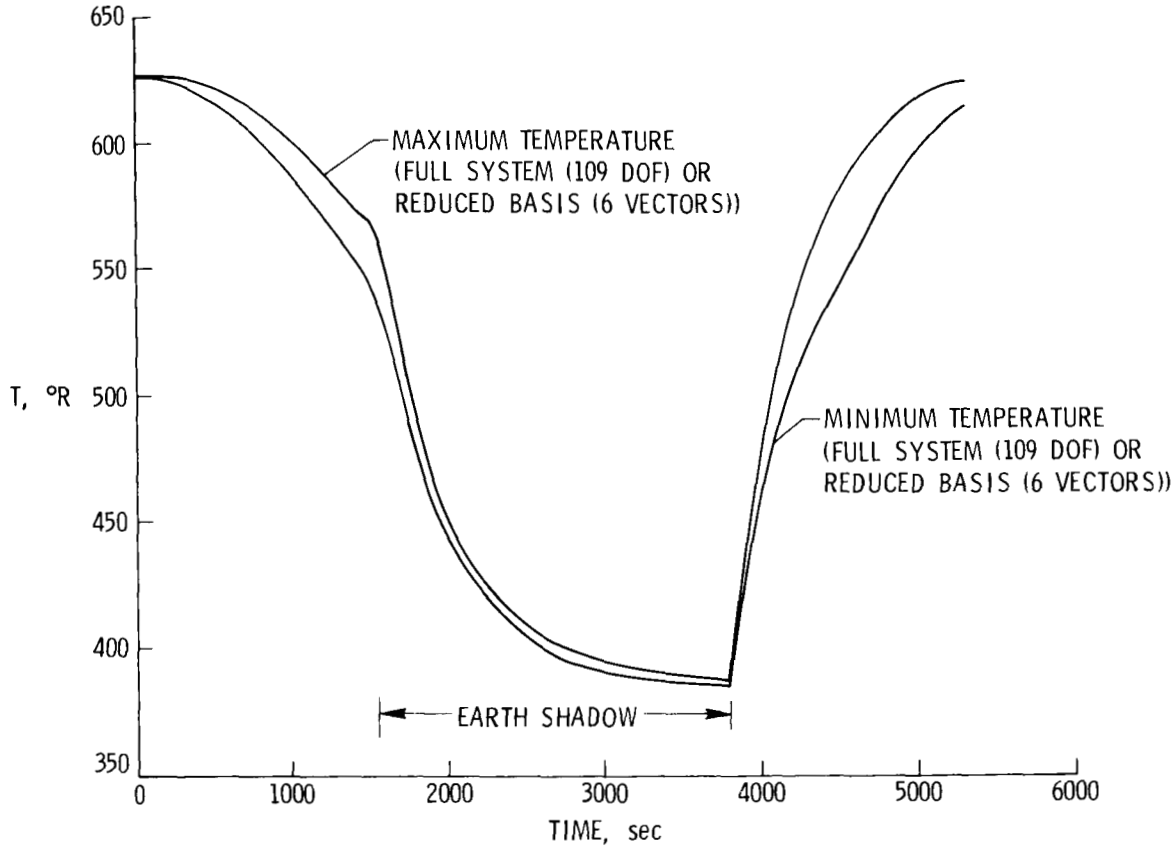

Figure 26. Reduction-method (using SS temperature profiles) and full-system temperatures for antenna problem.

1. Report No. NASA TP-2373	2. Government Accession No.	3. Recipient's Catalog No.
4. Title and Subtitle REDUCTION METHOD FOR THERMAL ANALYSIS OF COMPLEX AEROSPACE STRUCTURES		5. Report Date January 1985 6. Performing Organization Code 506-53-53-07
7. Author(s) Charles P. Shore		8. Performing Organization Report No. L-15777 10. Work Unit No.
9. Performing Organization Name and Address NASA Langley Research Center Hampton, VA 23665		11. Contract or Grant No.
12. Sponsoring Agency Name and Address National Aeronautics and Space Administration Washington, DC 20546		13. Type of Report and Period Covered Technical Paper 14. Sponsoring Agency Code
15. Supplementary Notes		

16. Abstract

A reduction method which combines classical Rayleigh-Ritz modal superposition techniques with contemporary finite-element methods is applied to transient nonlinear thermal analysis of aerospace structures. The essence of the method is the use of a few thermal modes from eigenvalue analyses as basis vectors to represent the temperature response in the structure. The method is used to obtain approximate temperature histories for a portion of the Shuttle orbiter wing subject to reentry heating and for a large space antenna reflector subject to heating associated with a low Earth orbit. Results are presented to show that the reduction method has excellent potential for significant size reduction for radiation-dominated problems such as the antenna reflector. However, for conduction-dominated problems such as the Shuttle wing, especially those with complex spatial and temporal variations in the applied heating, additional work appears necessary to find alternate sources of basis vectors which will permit significant problem size reductions.

17. Key Words (Suggested by Author(s)) Thermal analysis Reduction methods Nonlinear conduction Radiation Heat transfer	18. Distribution Statement Unclassified—Unlimited Subject Category 34

19. Security Classif. (of this report)	20. Security Classif. (of this page)	21. No. of Pages	22. Price
Unclassified	Unclassified	29	A03

For sale by the National Technical Information Service, Springfield, Virginia 22161

NASA-Langley, 1985

3 2 1U,D, 850103 S00161DS
DEPT OF THE AIR FORCE
ARNOLD ENG DEVELOPMENT CENTER(AFSC)
ATTN: LIBRARY/DOCUMENTS
ARNOLD AF STA TN 37389